

## THE EFFECT OF CALCIUM CARBONATE (CaCO<sub>3</sub>) NANOPARTICLES ON THE FLOW THROUGH A PENTAGON SPIRAL PIPE

Yanuar<sup>1,\*</sup>, M. A. Talahatu<sup>1</sup>, Sealtial Mau<sup>1</sup>, Kurniawan T. Waskito<sup>1</sup>, Winda Wulandari<sup>1</sup>

<sup>1</sup>*Department of Mechanical Engineering, Faculty of Engineering, Universitas Indonesia, Kampus UI Depok, Depok 16424, Indonesia*

(Received: January 2017/ Revised: May 2017 / Accepted: October 2017)

### ABSTRACT

CaCO<sub>3</sub> is friendly to both the environment and humans. For this reason, it is suitable to be applied in fluid transportation to enable more efficient flow. The objective of this study was to investigate the effect of CaCO<sub>3</sub> on the flow in a pentagon spiral pipe. The working fluid was circulated into the test pipe with constant pressure by the compressor. The working fluid was produced by mixing pure water with CaCO<sub>3</sub> nanoparticles, which have average diameter of 100 nm, in the concentration ratios of 100 ppm, 300 ppm and 500 ppm. The test pipe was a pentagon spiral pipe with the ratio P/Do 7.1, and a circular pipe with a 4 mm inner diameter was used for comparison. The highest drag reduction (DR) that occurred in the spiral pipe was 35% around Re'  $4 \times 10^4$  with nanofluids concentration of 500 ppm, while the highest DR in the circular pipe was of 26% around Re'  $4 \times 10^4$ . The results show that increasing the percentage of solid particles affects the properties of the working fluid, such as viscosity, density, pressure drop and DR. The effects of the change in fluid properties were also taken into account. These affect the damping phenomena in the near wall region, which gives friction factor reduction. Another benefit of the spiral pipe is that it prevents the sedimentation of nanoparticles.

*Keywords:* Calcium carbonate; Drag reduction; Nanofluids; Pentagon spiral pipe; Pressure drop

### 1. INTRODUCTION

Various methods are being developed, both theoretically and experimentally, in order to further improve the performance of fluid transportation (Cunha & Andreotti, 2007). One of the methods is the application of nanofluids application, for example in refrigeration systems (Pamitran et al., 2016). Energy consumption in pipelines can be achieved using two methods, active control and passive control. The passive control method is applied by modifying the structure of the wall surface, while the active control method involves adding a number of additives into the working fluid in order to reduce the drag force (Pouranfard et al., 2014). The characteristics of silica slurry flow in a spiral pipe with a 1 mm mean diameter have previously been studied (Yanuar et al., 2015).

Numerous studies conducted in the past few decades have focused on analyzing drag reduction (DR) in the pipeline. Indeed, Toms (1948) carried out a study using poly ethylene oxide, and found more than 50% DR in piping. Many researchers have studied DR using nanoparticles (Pouranfard et al., 2014; Kristiawan & Akmal, 2015), polymers (Yanuar et al., 2012; Yanuar et al., 2015), surfactants (Tamano et al., 2015) and fibers (Ogata & Warashina, 2014). The use of nanoparticles to reduce drag can change the characteristics of the working fluid, such as density,

---

\*Corresponding author's email: yanuar@eng.ui.ac.id, Tel: +62-21-7270029, Fax: +62-21-7270028  
Permalink/DOI: <https://doi.org/10.14716/ijtech.v8i7.696>

viscosity and drag, without causing deposition in the flow. Increasing the concentration of nanoparticles in the working fluid can increase the viscosity, but does not cause a temporary pressure drop (Kristiawan & Akmal, 2015).

Research conducted with the aim of improving DR through the application of nanoparticles proved successfully by modifying the nanoparticles on the surface of the pipe wall to be less rough, so the flow will slip through the pipe and reduce the friction factor (Pouranfard et al., 2014).

The objective of this research was to investigate the effects of calcium carbonate ( $\text{CaCO}_3$ ) on the flow in a pentagon spiral pipe. This experiment used both a circular and spiral pipe. The efficiency of the working fluid flowing through the spiral pipe has its own advantages over the circular pipe. A pipe with a geometric spiral shape could increase the DR under some conditions, and can also avoid the deposition at low speed (Watanabe et al., 1984).

## 2. EXPERIMENTAL

The geometry and size of the pentagon spiral pipe are shown in Figure 1 and Table 1, respectively. The pentagon spiral pipe has aspect ratio  $P/D_o = 7.1$ . A circular pipe with a similar diameter was used for comparison in this experiment.

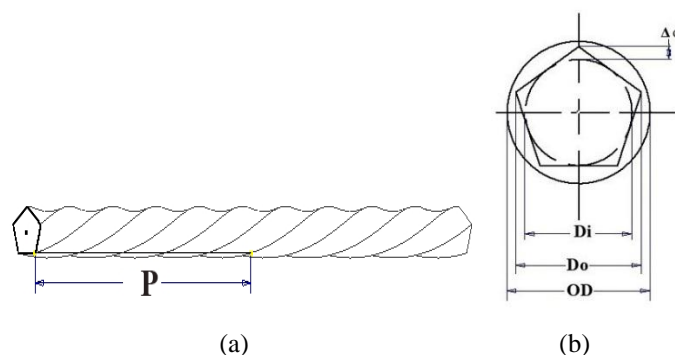


Figure 1 Geometry of pentagon spiral pipe: (a) Side view of pipe hollow; (b) Front view of pipe hollow

Table 1 Specification of geometry of test pipe

Test pipe	Di (mm)	Do (mm)	$\Delta d$ (mm)	P (Pitch)	P/Do
Circular	6.3	-	-	-	-
Spiral	5.25	8.55	3.3	60.7	7.1

The experimental set-up is shown in Figure 2. The length of the section tested is 900 mm, on both sides of which a pressure transducer is mounted. The distance from the inlet pipe to the high pressure tap is 1000 mm with the condition that the fluid had been fully developed. The pump used is a centrifugal pump with capacity 8 l/min. The working fluid was circulated in the test pipe with pressure from the compressor. In order to regulate the flow rate, a volt regulator was used to adjust the pump. The distance between the pressure taps is 900 mm. As a comparison to the spiral pipe, the test was also conducted using a circular pipe with inner diameter 6.3 mm and length equal to the spiral pipe. A pressure transducer was used to calculate the different pressures in the test section. A flow meter was used to measure the flow rate and a glass measurement was used for comparison with the flow meter. The pressure tank has a capacity of up to 8 liters.

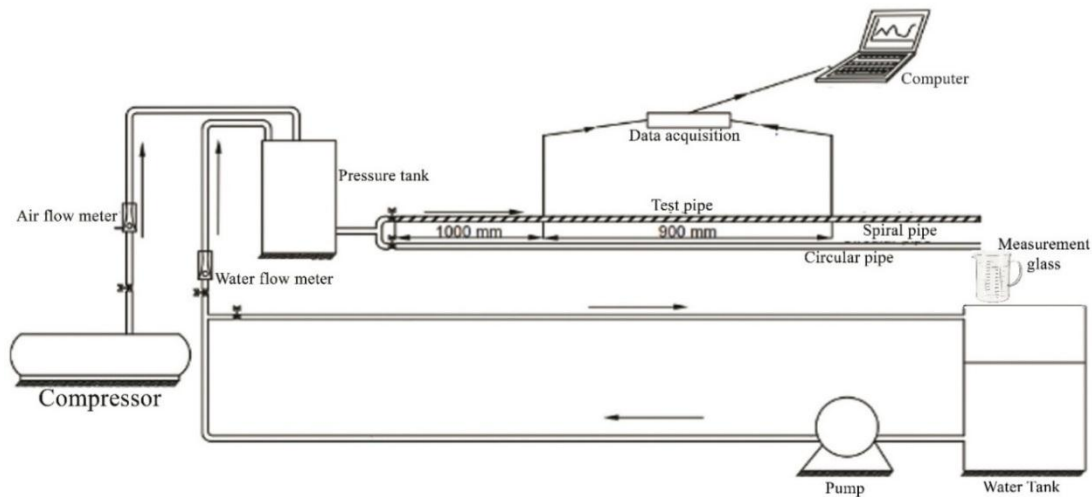


Figure 2 Experimental set-up

In this research, the  $\text{CaCO}_3$  nanoparticles have a 100 nm mean diameter with the concentrations 100 ppm, 300 ppm and 500 ppm, and are compared with water and mixed for about 120 minutes.

### 2.1. Experimental Validation

The experimental set-up was validated with the preliminary data without nanoparticles to approach the friction factor from the Hagen–Poiseuille equation for laminar flow and the Blasius equation for turbulent flow as follows:

$$f = \frac{64}{\text{Re}} \quad (1)$$

$$f = \frac{0.3164}{\text{Re}^{0.25}} \quad (2)$$

Both of these equations were used because the fluid used in this test was Newtonian fluid. For Newtonian flow, the Reynolds number is calculated with a constant viscosity, or simply depends on the temperature, without relying on the influence of shear stress.

$$\text{Re} = \frac{\rho U D_o}{\mu} \quad (3)$$

where  $\text{Re}$  is the Reynolds number,  $\rho$  is the density,  $U$  is the flow velocity,  $D_o$  is the maximum outer diameter, and  $\mu$  is the dynamic viscosity. Figure 3 shows the validation of the experimental set-up with the Hagen–Poiseuille and the Blasius equation.

### 2.2. Rheological Models

The relationship between the Reynolds number and the friction coefficient was plotted on a Moody diagram.

The change in viscosity of the non-Newtonian fluid is due to shear strain,  $\gamma$ . Apparent viscosity is associated with an absolute value of shear stress,  $\tau$ :

$$\tau = K \left( \frac{\partial u}{\partial y} \right)^n = K (\gamma)^n \quad (4)$$

where  $K$  is the consistency coefficient, and  $n$  is the power-law index.

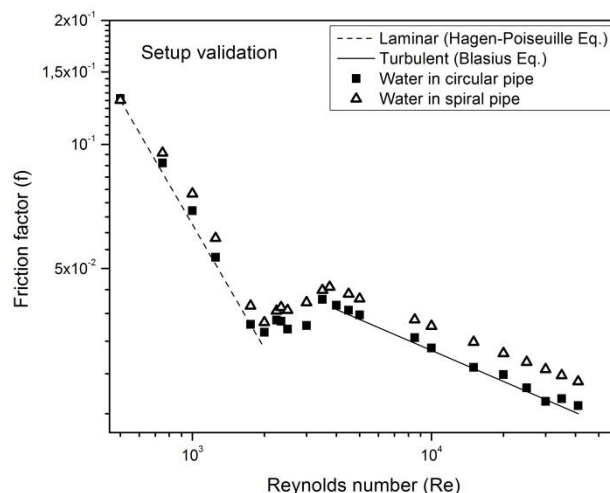


Figure 3 Validation of experimental set-up

For  $n = 1$ , that is for Newtonian behavior,  $K = \mu$  corresponds to the Newtonian viscosity.

$$\tau = \frac{D\Delta P}{4L} \tag{5}$$

$$\gamma = \frac{8U}{D} \tag{6}$$

where  $\Delta P$  is the pressure drop, and  $L$  is the length of pipe.  $n < 1$  for the pseudoplastic model and  $n > 1$  for the dilatant model. By obtaining the shear stress and flow rate of the fluid, the power-law index,  $n$ , can be determined using the following equation:

$$n = \frac{\text{Log} \frac{\tau_1}{\tau_2}}{\text{Log} \frac{\gamma_1}{\gamma_2}} \tag{7}$$

Figures 4 and 5 demonstrate the rheological behavior of the  $\text{CaCO}_3$  nanofluid. The shear stress increases with an increase in the shear rate and particle concentration. According to those flow curves, the characteristic of  $\text{CaCO}_3$  was a pseudoplastic model with a power-law index ( $n$ ) of 0.92, 0.90, and 0.89 for 100, 300, and 500 ppm, respectively.

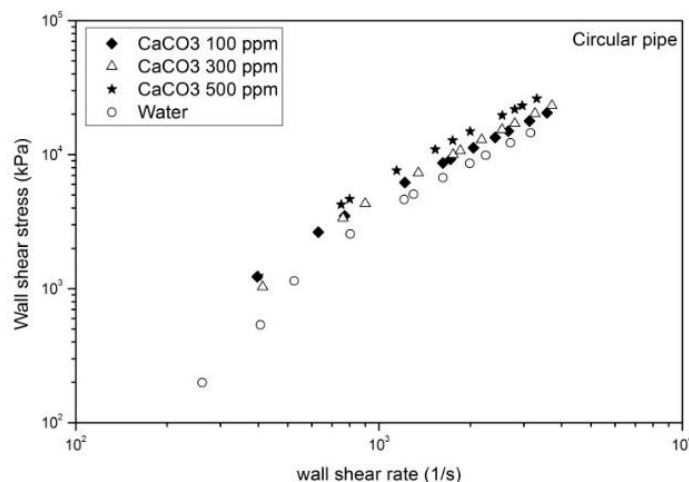


Figure 4 Comparison of wall shear rate with shear stress in circular pipe

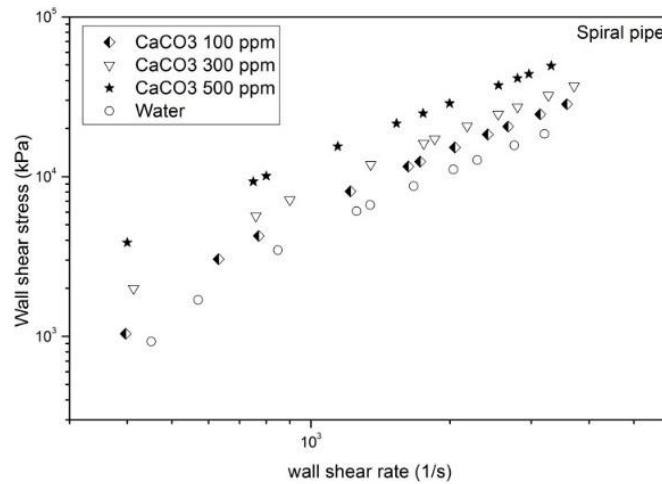


Figure 5 Comparison of wall shear rate with shear stress in pentagon spiral pipe

The comparison between the shear rate and shear stress shows that this fluid is a non-Newtonian fluid, so the non-Newtonian equations will be employed.  $Re'$ , the generalized Reynolds number, can be obtained from the following equation:

$$Re' = \frac{8n^n \rho D^n V^{2-n}}{2^n (3n+1)^n K} \tag{8}$$

The coefficient of friction factor,  $f$ , can be obtained using the Darcy Equation:

$$f = \left( \frac{2Do}{\rho LU^2} \right) \Delta P \tag{9}$$

where  $f$  is the coefficient of friction.

Drag reduction (DR) in the pipe can be obtained using the following equation:

$$\% DR = \left| \frac{f_w - f_N}{f_w} \right| \times 100 \tag{10}$$

where,  $f_w$  is the coefficient of water friction factor, and  $f_N$  is the nanofluid friction factor.

### 3. RESULTS AND DISCUSSION

#### 3.1. Friction Factor

During this study, the friction factor became the main focus to be discussed. The following graphs demonstrate the relationship between the generalized Reynolds number and the friction factor. Figures 6 and 7 show that the friction factor occurs in the circular pipe and spiral pipe after reaching  $1 \times 10^4$ . The focus of the analysis is in the turbulent region, while in the laminar flow, the addition of nanoparticles did not have a major effect on the friction factor, and increasing the generalized Reynolds number shows no tendency to increase DR.

In the turbulent region, the working fluid with CaCO<sub>3</sub> nanoparticles has a friction factor lower than that of pure water. Increasing the value of the generalized Reynolds number means increasing the turbulent intensity in the pipeline but the addition of nanoparticles enables the condition of the turbulent flow to become profit able. It is indicated that DR can be increased by decreasing the friction factor.

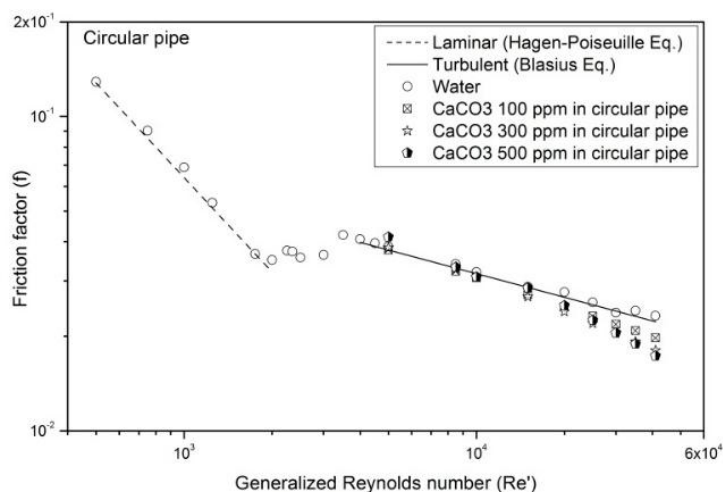


Figure 6 Generalized Reynolds number versus friction factor in circular pipe

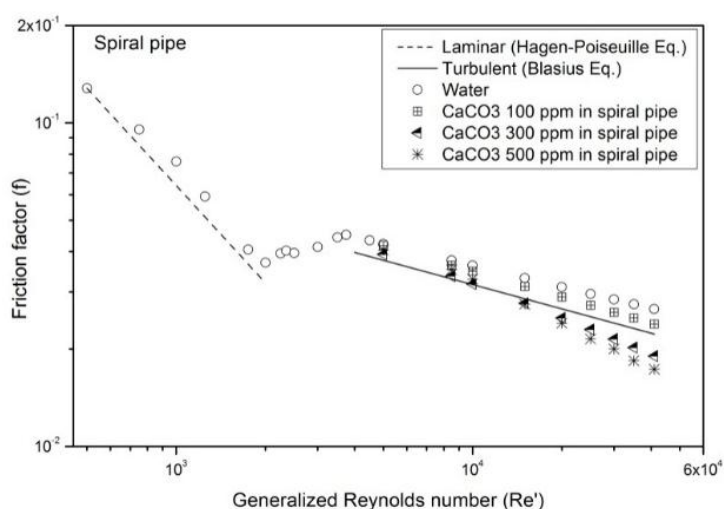


Figure 7 Generalized Reynolds number versus friction factor in pentagon spiral pipe

### 3.2. Drag reduction

In Figure 8, an increase in DR in both the circular pipe and the pentagon spiral pipe can be seen. The lowest DR of the CaCO<sub>3</sub> nanofluid is 100 ppm and the highest is 500 ppm. When the flow through the spiral pipe reaches the range  $Re' 3 \times 10^3$  to  $1.5 \times 10^4$ , the DR generated by 500 ppm nanofluid is lower than that of 300 ppm nanofluid. In this condition, it can be concluded that the fluid is in the transition toward the maximum value of DR.

In the circular pipe, for  $Re'$  range  $3 \times 10^3$  to  $1 \times 10^4$ , the highest DR is that of 100 ppm nanofluid. For  $Re'$  range  $1 \times 10^4$  to  $3 \times 10^4$ , this changes to the CaCO<sub>3</sub> nanofluid with 300 ppm. When  $Re'$  exceeds  $3 \times 10^4$ , the highest DR becomes the CaCO<sub>3</sub> nanofluid with 500 ppm. In certain  $Re'$  ranges showing transition, randomness was indicated by the third line on the graph for the circular pipe. Through this phenomenon, not all concentration ratios of nanofluid show the same benefits as others for all flow regions; some ranges of Reynolds number obtained different results with regard to DR.

DR occurs in the fluid mixture with nanoparticles due to the increase in viscosity and density; it affects the damping phenomena in the near wall region, which gives effect to the friction factor reduction. The damping effect becomes more beneficial with increasing turbulent intensity.

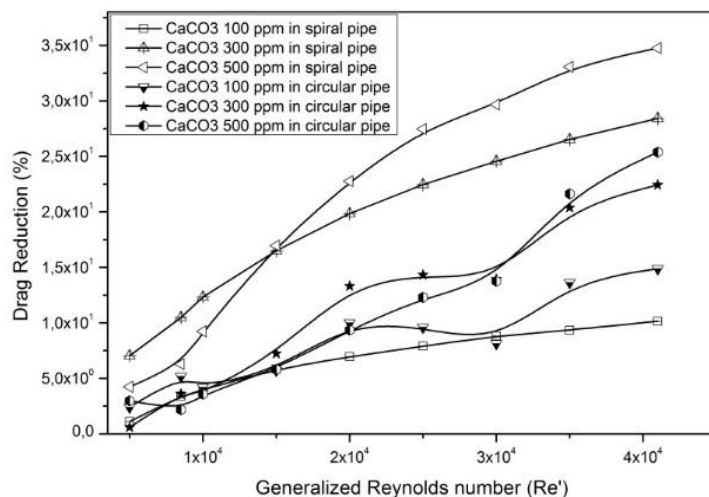


Figure 8 Generalized Reynolds number versus drag reduction

The comparison of the spiral pipe and the circular pipe shows that the highest DR occurs in the pentagon spiral pipe. DR was highest in this spiral pipe because it has more turbulent intensity, and a circumferential force caused by the geometry of the spiral pipe resulted in the fluid twisting, so that the friction between the wall and the working fluid was reduced. The increase in the value of DR in the circular pipe resulting from the application of nanoparticles is in accordance with the results of Pouranfard et al., 2014. For the spiral pipe, DR reaches its highest (35%) at  $Re'$   $4 \times 10^4$  with 500 ppm nanofluid, and for the circular pipe, DR is highest (26%) at  $Re'$   $4 \times 10^4$  with 500 ppm nanofluid.

#### 4. CONCLUSION

DR occurring in the pentagon spiral pipe and circular pipe varies depending on the mixture of  $\text{CaCO}_3$  nanoparticles and the value of  $Re'$ . The highest DR that occurs in the spiral pipe is 35% for  $Re'$   $4 \times 10^4$  with nanofluid concentration of 500 ppm, while the highest in the circular pipe is 26% at the  $Re'$   $4 \times 10^4$ . The highest DR value is exhibited in the spiral pipe because it has more turbulent intensity, and the geometry of the spiral pipe generates circumferential flow resulting in the working fluids twisting at a certain Reynolds number. The effect of the change in fluid properties also affects the damping phenomena in the near wall region, which gives effect to friction factor reduction.

#### 5. REFERENCES

- Cunha, F., Andreotti, M., 2007. A Study of the Effect of Polymer Solution in Promoting Friction Reduction in Turbulent Channel Flow. *Journal of Fluids Engineering*, Volume 129(4), pp. 491–505
- Kristiawan, B., Kamal, S., 2015. A Modified Power Law Approach for Rheological Titania Nanofluids Flow Behavior in a Circular Conduit. *Journal of Nanofluids*, Volume 4(2), pp. 187–195
- Ogata, S., Gunawan, Warashina, J., Yanuar, 2014. Drag Reduction of a Pipe Flow using *Nata de Coco* Suspensions. *Advances in Mechanical Engineering*, Volume 2014, pp. 1–8
- Pamitran, A.S. Putra, N. Budiono, H.D.S., 2016. Thermofluids on Renewable Energy, Refrigeration and Air Conditioning, and Flame, and Combustion. *International Journal of Technology*, Volume 7(2), pp 185–188

- Pouranfard, A., Mowla, D., Esmaeilzadeh, F., 2014. An Experimental Study of Drag Reduction by Nanofluids through Horizontal Pipe Turbulent Flow of a Newtonian Liquid. *Journal of Industrial and Engineering Chemistry*, Volume 20(2), pp. 633–637
- Tamano, S., Ikarashi, H., Morinishi, Y., Taga, K., 2015. Drag Reduction and Degradation of Nonionic Surfactant Solutions with Organic Acid in Turbulent Pipe Flow. *Journal of Non-Newtonian Fluid Mechanics*, Volume 215, pp.1–7
- Toms, B.A., 1948. Some Observations on the Flow of Linear Polymer Solutions through Straight Tubes at Large Reynolds Numbers. *In: Proceedings of the 1<sup>st</sup> International Congress on Rheology*
- Watanabe, K., Iwata, T., Kato, H., 1984. *Flow in a Spiral Tube: 2<sup>nd</sup> Report, Hydraulic Transport of Solids in a Horizontal Pipe*. Bulletin of JSME. Volume 27(230), pp. 1682–1688
- Yanuar, Gunawan, Baqi, M., 2012. Characteristics of Drag Reduction by Guar Gum in Spiral Pipes. *Jurnal Teknologi UTM*, Volume 58(2), pp. 95–99
- Yanuar, Gunawan, Sapjah, D., 2015. Characteristics of Silica Slurry Flow in a Spiral Pipe. *International Journal of Technology*, Volume 6(6), pp. 916–923
- Yanuar, Waskito, K.T., Gunawan, Budiarmo, 2015. Drag Reduction and Velocity Profiles Distribution of Crude Oil Flow in Spiral Pipes. *International Review of Mechanical Engineering*, Volume 9(1), pp. 1–10